Automatic segmentation of a meningioma using a computational technique in magnetic resonance imaging

Segmentación automática de un meningioma usando una técnica computacional en imágenes de resonancia magnética

Miguel Vera MSc, PhD[1,2], https://orcid.org/0000-0001-7167-6356, Yoleidy Huérfano MSc[2], https://orcid.org/0000-0003-0415-6654, Ángel Valentín Molina MSc[3], https://orcid.org/0000-0001-9604-7222, Oscar Valbuena MSc[4], https://orcid.org/0000-0003-3080-8839, Marisela Vivas MSc, PhD[5], https://orcid.org/0000-0002-8941-4562, María Cuberos MSc, PhD[6], https://orcid.org/0000-0002-5235-552X, Williams Salazar MD[7], https://orcid.org/0000-0001-5669-6105, María Isabel Vera BSc[7], https://orcid.org/0000-0003-1135-6283, Maryury Borrero MSc[1], https://orcid.org/0000-0003-3025-1321, Carlos Hernández MSc[1], https://orcid.org/0000-0001-8906-1982, Doris Barrera MSc[1], https://orcid.org/0000-0002-6443-6757, Luis Javier Martínez PhD[3], https://orcid.org/0000-0003-0917-9847, Juan Salazar MSc[1], https://orcid.org/0000-0001-6826-203X, Elkin Gelvez MSc[1], https://orcid.org/0000-0001-5157-3341, Yudith Contreras MSc[1], https://orcid.org/0000-0003-4358-730X, Frank Sáenz MSc[8], https://orcid.org/0000-0001-9604-7220*

[1]Universidad Simón Bolívar, Facultad de Ciencias Básicas y Biomédicas, Cúcuta, Colombia.

**E-mail de correspondencia: m.avera@unisimonbolivar.edu.co*

[2]Grupo de Investigación en Procesamiento Computacional de Datos (GIPCD-ULA), Universidad de Los Andes-Táchira, Venezuela.

[3]Grupo de Investigación en Ingeniería Clínica - HUS (GINIC-HUS), Vicerrectoría de Investigación, Universidad ECCI.

[4]Grupo de Investigación en Educación Matemática, Matemática y Estadística (EDUMATEST), Facultad de Ciencias Básicas, Universidad de Pamplona.

[5]Universidad Simón Bolívar, Departamento de Ciencias Sociales y Humanas, Cúcuta, Colombia.

[6]Universidad Simón Bolívar, Facultad de Administración y Negocios, Cúcuta, Colombia.

[7]Servicio de Neurología, Hospital Central de San Cristóbal-Táchira, Venezuela.

[8]Universidad Simón Bolívar, Facultad de Ingeniería, Cúcuta, Colombia.

Abstract

Through this work we propose a computational technique for the segmentation of a brain tumor, identified as meningioma (MGT), which is present in magnetic resonance images (MRI). This technique consists of 3 stages developed in the three-dimensional domain: pre-processing, segmentation and post-processing. The percent relative error (*PrE*) is considered to compare the segmentations of the MGT, generated by a neuro-oncologist manually, with the dilated segmentations of the MGT, obtained automatically. The combination of parameters linked to the lowest *PrE*, provides the optimal parameters of each computational algorithm that makes up the proposed computational technique. Results allow reporting a *PrE* of 1.44%, showing an excellent correlation between the manual segmentations and those produced by the computational technique developed.

Keywords*:* Magnetic resonance brain imaging, Brain tumor, Meningioma, Computational technique, Segmentation.

Resumen

Este trabajo propone una técnica computacional para la segmentación de un tumor cerebral, identificado como meningioma (MGT), que está presente en imágenes de resonancia magnética (MRI). Esta técnica consta de 3 etapas desarrolladas en el dominio tridimensional: preprocesamiento, segmentación y postprocesamiento. El porcentaje de error relativo (PrE) se considera para comparar las segmentaciones de la MGT, generadas por un neurooncólogo de forma manual, con las segmentaciones dilatadas de la MGT, obtenidas automáticamente. La combinación de parámetros vinculados al PrE más bajo proporciona los parámetros óptimos de cada algoritmo computacional que conforma la técnica de cálculo propuesta. Los resultados permiten informar un PrE de 1.44%, mostrando una excelente correlación entre las segmentaciones manuales y las producidas por la técnica computacional desarrollada.

Palabras clave: Imágenes cerebrales por resonancia magnética, Tumor cerebral, Meningioma, Técnica computacional, Segmentación.

Introduction

The segmentation of anatomical structures of the human brain, present in images acquired by any imaging modality, constitutes the starting point for the diagnosis of a large number of diseases or pathologies affecting the brain. Among these are brain tumors, which originate from various cell lines and are classified according to several criteria[1]. One of them is where in the body they are generated. In this sense, they can be classified into two groups: a) Primary tumors. Space-occupying lesions (SOLC) that start in the brain and tend to remain there. b) Secondary tumors. SOLC that originate in other sites of the human body and spread and/or infiltrate the brain, as metastasis. The most frequent metastases come from cancers in skin, lungs and breast[2,3].

In this context, meningiomas represent approximately 34% of all primary brain tumors. Generally, this type of tumor is diagnosed in adults over 60 years old and its incidence seems to increase with age. Meningiomas are rarely found in children. Their incidence in women almost doubles that in men[3].

The World Health Organization (WHO)[4] uses the degree of malignancy of the tumor as a criterion to classify primary tumors into four grades. According to this classification, tumors labeled with grades I and II are generally benign; while those classified in grades III and IV are considered malignant. Normally, patients with primary grade I brain tumors have a longer survival than those with grade IV tumors[1,2,3]. For the

present study, the tumors reported in the literature as meningiomas are of special interest.

Meningiomas arise in the meninges, three thin layers of tissue that wrap the brain and the spinal cord. These tumors usually grow inward causing pressure on the brain or spinal cord, but also can grow outward, towards the skull, causing its thickening. The majority of meningiomas are benign tumors of slow growth. Some of them contain cysts, calcifications or concentrated groupings of blood vessels[3]. According to WHO[4], the meningiomas can be located in the context illustrated in figure 1.

Figure 1. Block diagram with a classification linked to the brain tumor considered in the present work.

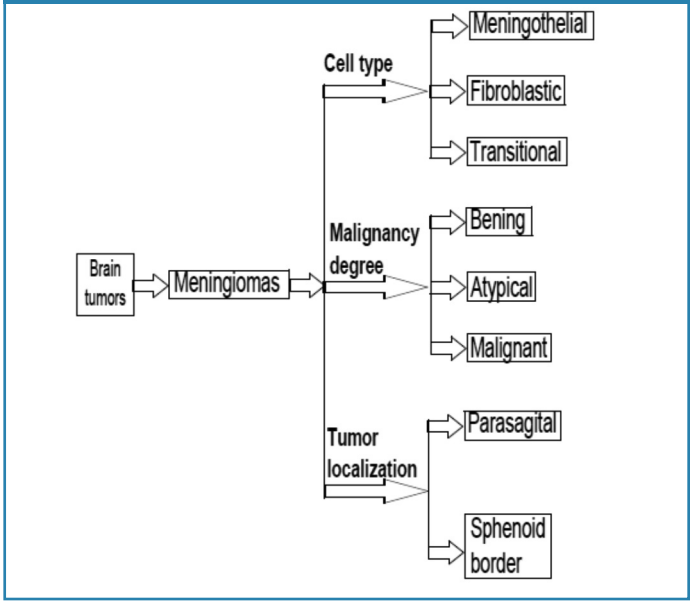

Additionally, table 1 presents important information, considering references[3,5], that allow characterization of meningiomas.

Table 1. Main features about meningiomas.

Causes	Symptoms	Diagnostic techniques	Medical treatment
22-chromosome abnormality.	Headache	Neurological examination	Surgery
Extra copies of EGFR* and PDGF**.	Muscle weakness in upper or lower extremities	MRI or CT	Radiotherapy
Breast cancer, neurofibromatosis type 2. (Radiation)	Visual blur and seizures	Angiography Arteriography	Immunotherapy
Consumption of hormones linked to sexual hormonal disorders	Humor changes	Biopsy	Progesterone, EGFR and PDGF Inhibitors

*EGFR: epidermal growth factor receptors.

**PDGF: platelet-derived growth factor.

Cerebral digital neuroimages are usually accompanied by various imperfections such as noise[8,9,10] and artifacts[8] which affect the quality of information associated with the anatomical structures that make up these images. These imperfections become real challenges, when computational strategies are implemented to generate the morphology (normal or abnormal) of the mentioned structures[8]. By way of example, figure 2, generated by magnetic resonance images (MRI), illustrates the presence of Rician noise, the stair artifact, and the low contrast between brain structures and the meningioma (structure with red cross in its center).

Figure 2. Axial views of brain MRI in which one can observe Rician noise, low contrast between lobular structures and the MGT (Red cross).

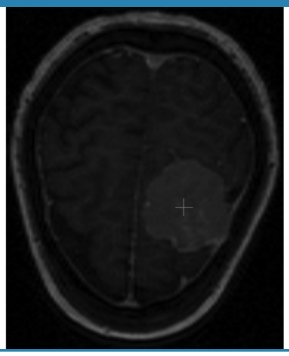

Reviewing the state of the art regarding tumor segmentation, the works described below were found. Sanjuán et al.[9] proposed a technique for brain tumors classification, including meningiomas, based on an MRI modality of automatic segmentation with refined patient-specific priors. This technique identified the tumors in good agreement with the manual segmentation (area under the ROC curve = 0.97 ± 0.03).

Similarly, Hsieh et al.[10], proposed an automatic segmentation of meningioma from 30 non-contrasted brain T1 and T2 -weighted MR images integrating fuzzy clustering and region growing technique. The aims of this study were: a) To locate tumors in the images. b) To detect those situated in the midline position of the brain. The parameters percent match and correlation ratio show a close match between ground truth and the present their study's system, as well as a fair level of correspondence.

Kauss et al.[11], present a system based on adaptive template moderated classification for the automated segmentation of 3D MRI brain data sets of patients with brain tumors (meningiomas and low grade gliomas). In a validation study of 13 patients with brain tumors, the segmentation results of the automated method are compared to manual segmentations carried out by 4 independent trained human observers. It is shown that the automated method segments brain and tumor with accuracy comparable to the manual method.

In our present work, a computational technique (CT) is proposed for the segmentation of a MGT, present in a database formed by three-dimensional brain images of MSCT. This technique involves the stages of pre-processing, segmentation and post-processing Also, percent relative error (*PrE*)[6] is used to compare segmentations of the MGT obtained automatically with those obtained manually.

Materials and methods

Description of the databases

The database (DB) used was provided by the Central Hospital of San Cristóbal-Táchira-Venezuela. It was acquired through the MRI modality and consists of three-dimensional images (3D), corresponding to the anatomical structures present in the head of a female patient. Numerical characteristics are presented on table 2.

Table 2. General characteristics of the database considered in the present work.

DB Label	Voxels number	Voxels dimensions (mm^3)	Age (years)
DB1	256x256x124	0.9375 x 0.9375x 1.5	55

For comparison, a manual segmentation is available, generated by a neuro-oncologist, corresponding to the LGG present in the DB considered. This segmentation represents the ground truth that will serve as a reference to validate the results.

Description of the proposed computational technique, for the automatic segmentation of the LGG.

Figure 3 shows a schematic diagram synthesizing the methods that make up the proposed technique, to segment the tumor.

Figure 3. Block diagram of the CT proposed for the segmentation of the LGG.

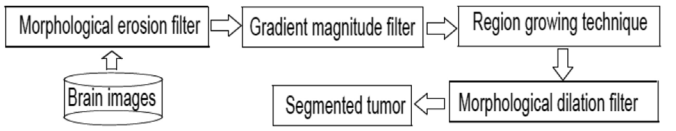

Pre-processing Stage

In the block diagram, presented in figure 3, this stage corresponds to the techniques: Erosion and Gradient magnitude filter. They are described presently:

- Morphological Erosion Filter (MEF):

Since mathematical morphology is based on set theory, the objects present in an image may be treated as sets of points[12]. Generally, it is possible to define operations between two sets, one consisting of elements belonging to the aforementioned objects and another set called structuring element (SE)[13]. SEs can be visualized as neighborhoods of the element under study, which have variable morphology[14].

In practice, Mathematical morphology is implemented through various morphological filters whose basic operators are erosion and dilation[13,14]. These operators are non-linear spatial filters that can be applied to binary, grayscale or color images.

In particular, the erosion (Θ) of a two-dimensional image (I), composed of gray levels, using a two-dimensional SE, is defined by Equation 1[14,15].

$$(I \ominus SE)(x,y) = \min_{(s,t)\,\epsilon\,B}[I(x+s,y+t) - SE(s,t)]. \qquad (1)$$

Where: *min* the minimum gray level contained in *SE, (s, t)* defines the size of the *SE* and *(x, y)* represents the position of the pixel under study.

According to equation 1, to apply the filter or morphological erosion operator the image considered with an SE or neighborhood, of arbitrary size, is covered, replacing the gray level of each of the elements of such an image by the level of gray minimum, contained in the aforementioned neighborhood. For purposes of the present work, a cubic structuring element was considered and the size of said SE is left as a parameter to control the performance of the MEF.

- Gradient Magnitude Filter (GMF):

The role of this filter is to detect the edges of the structures present in the images (I). The magnitude of the gradient is often used in image analysis, mainly to identify the contours of objects and the separation of homogeneous regions[16]. Edge detection is the identification of significant discontinuities in the level of gray or color images[17]. This technique calculates the magnitude of the gradient using the first directional partial derivatives of an image.

- Binary Morphological Dilation Filter (MDF):

In order to compensate the effect produced by the morphological erosion filter, the application of a morphological dilation filter (MDF) is considered, taking into account the binary image obtained by RG. The effect of morphological dilation is to enlarge the regions of the maximum intensity image. In particular, the dilation (⊕) of a two-dimensional binary image (Ib), using a bidimensional structuring element (B), is defined as the result of operating the Ib with the values of the SE under the logical operation OR[14]. For the purposes of this work, a cubic structuring element was considered and the size of said SE is left as a parameter to control the performance of the dilatation process.

Segmentation Stage

- Computer intelligence operators: Support Vector Machines (SVM).

Support vector machines (SVM) are paradigms that undergo training and detection processes, and are based on both the Vapnik-Chervonenkis learning theory and the minimization principle that considers structural risk[18]. SVM can be considered as classification and functional approach tools[19,20].

A variant of the SVM, called the least squares vector support machine (LSSVM), can be obtained using robust statistics, Fisher discriminant analysis and replacing the system of inequations that govern the SVM, by an equivalent system of linear equations, which can be solved more efficiently[21,22]. Additionally, unlike other learning-based classification systems such as artificial neural networks (NN), LSSVMs use the criterion of minimization of structural risk, which raises the generalization capacity of the aforementioned machines to optimum levels, making it possible for LSSVM perform adequately in the validation process, surpassing NN in this aspect, which uses empirical risk[23].

In this work, the location of the seed voxel, to initialize the segmentation technique called region growth (RG)[13], is calculated using LSSVM. There are several functions that can be considered to construct the decision surface that allow the vector support machines to identify the seed. For purposes of the present work, a Gaussian radial base function (RBF) is considered and, therefore, a formulation is obtained that depends on the hyperparameters, identified as: a) Error penalty parameter (γ). b) Parameter to control the selectivity (σ^2) of the LSSVM.

In this sense, the LSSVMs call for a process of tuning of such hyperparameters. Theoretically, both parameters can assume values belonging in the range of real numbers comprised in between 0 and infinity[21,22]. The tuning process is necessary because it is very difficult to know, a priori, the combination of values that will generate optimal results when the LSSVM carry out the training and validation processes.

Additionally, to automatically identify the coordinates of the seed voxel, the following procedure was implemented:

i) A size reduction technique, based on bicubic interpolation, optimal reduction factor, is applied to match the one obtained in[6]. This allows to generate sub-sampled images of 64x64 pixels from filtered images of 512x512, that is, the mentioned factor is 8.

ii) A neurosurgeon selects, on the sub-sampled image, a reference point (P1) given by the centroid of the layer containing the maximum blood pool occupied by the MGT. For this point, the manual coordinates that unambiguously establish their spatial location in each considered image are identified.

iii) An LSSVM is implemented to recognize and detect point P1. For this, the processes of:

a) **Training**. Training circle circular neighborhoods of 10 pixels, manually traced by a neurosurgeon, containing both point P1 (markers) and regions not containing P1 (no markers) are selected as a training set. For the markers, the center of their respective neighborhoods coincides with the manual coordinates of P1, previously established.

Such neighborhoods are constructed on the axial view of a sub-sampled image of 64x64 pixels. The main reason why a single image is chosen, for each reference point, is because it is desired to generate a LSSVM with a high degree of selectivity, which detects only those pixels that have a high degree of correlation with the training pattern.

Then each neighborhood is vectorized and, considering its gray levels, the attributes mean, variance, standard deviation and median, are calculated. Thus, both markers and non-markers are described by vectors (**Va**) of statistical attributes, given by: **Va** = [mean, variance, standard deviation and median].

Additionally, the LSSVM is trained considering the vectors **Va** as a training pattern and intoning the values of the parameters that control its performance, γ and σ^2. This approach, based on attributes, allows the LSSVM to do its work with greater efficiency, than when using the larger vector-based approach, which only considers the gray level of the elements of an image.

The training set is constructed with a ratio of 1:10, which means that 10 non-markers are included for each marker. The tag +1 is assigned to the class made up of the markers; while the -1 tag is assigned to the class of non-markers, that is, the training work is done based on a binary LSSVM.

During training, a classifier with a decision boundary is generated to detect LSSVM entry patterns as markers or non-markers. Subsequently, due to the presence of false positives and negatives, a process is applied that allows incorporating into the training set the patterns that the LSSVM initially classifies inappropriately.

In this sense, it was considered a toolbox called LS-SVM-LAB and the Matlab15 application to implement an LSSVM classifier based on a radial base Gaussian kernel with parameters σ^2 and γ.

b) **Detection**. The trained LSSVMs are used to detect *P1*, in images not used during training. To do this, a trained LSSVM looks for this reference point, in the axial view, from the first to the last image that makes up each of the 7 databases considered.

The validation process carried out with LSSVM allows the automatic identification of coordinates for P1 which are multiplied by a factor of 8 units, in order to be able to locate them in the images of original size. In this way, the aforementioned coordinates are used to establish the exact location of the seed voxel required by the RG for its initialization.

Finally, as a synthesis, figure 4 illustrates the process followed to locate the seed voxel in the databases considered.

Figure 4. Synthetic diagram that illustrates the operability of the LSSVM for the detection of the seed voxel coordinates.

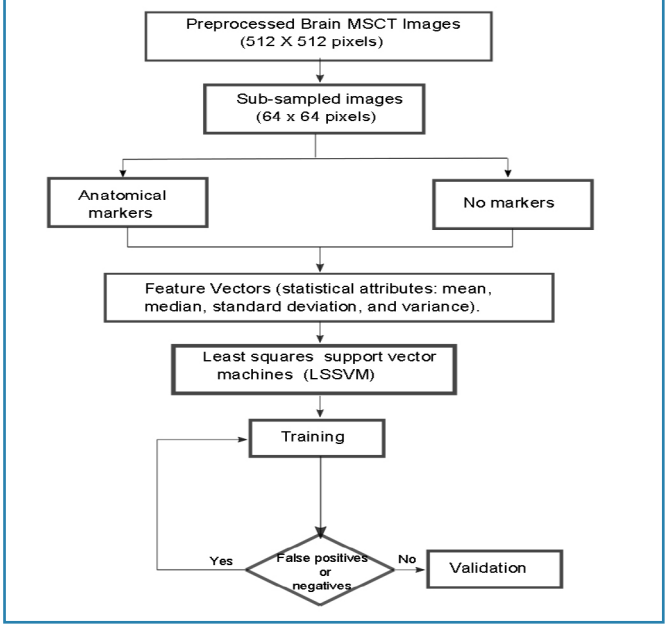

- Region growing (RG).

The region growing is an unsupervised clustering technique, which performs an iterative process that attempts to characterize each of the classes, according to the similarity between the voxels that integrate each of them and thus perform the segmentation[13]. The RG method allows you to group the pixels or voxels belonging to the objects that make up an image according to a predefined criterion. The RG requires a "seed" point which can be selected, manually or automatically, to extract all the pixels connected to seed[13].

To apply the RG, to the pre-processed images, the following considerations were made: a) The initial neighborhood, which is constructed from the seed, is assigned a cubic shape whose side depends on an arbitrary scalar *r*. The *r* parameter requires a tuning process. b) As a pre-defined criterion, modeling is chosen through Equation 2.

$$|I(x) - \mu| < m\sigma \qquad (2)$$

Where: I(x) is the intensity of the seed voxel, μ and σ the arithmetic mean and the standard deviation of the gray levels of the initial neighborhood and *m* a parameter that requires tuning.

Tuning process: Obtaining optimal parameters

The adequate performance of the proposed technique requires obtaining optimal parameters for each of the algorithms that comprise it. To do this, using DB1 as a reference, modify the parameters associated with the technique you wish to intone by systematically going through the values belonging to certain ranges, as described below.

- Dilation and erosion filters have the size of the observation window as a parameter. In order to reduce the number of possible combinations, an isotropic approach was considered to establish the range of values, which control the size of the aforementioned window, which is given by the odd combinations, given by the following ordered lists: (1,1,1), (3,3,3), (5,5,5), (7,7,7) and (9,9,9).

- The parameters of the LSSVM, σ^2 and γ, are toned assuming that the cost function is convex and developing tests based on the following steps:

➢ For the tuning of parameter γ the value of σ^2 is arbitrarily set and values are systematically assigned to the parameter γ. The value of σ^2 is initially set at 2.5. Then, γ is varied considering the range [0,100] by steps of 0.25.

➢ An analogous process is applied to intone the parameter σ^2, that is, γ is assigned the optimal value obtained in the previous step and a step size of 0.25 is considered to assign to σ the range of values contained in the interval [0.50].

 The optimal parameters of the LSSVM are those values of γ and σ^2 that correspond to the relative minimum percentage error, calculated considering the manual coordinates of the reference seed, established by the neurosurgeon and the automatic ones generated by the LSSVM.

- During the RG parameters tuning process, each one of the automatic segmentations of the MGT corresponding to the DB1 described, is compared with the manual segmentations of the MGT generated by a neurosurgeon, considering the *PrE*. The optimal values for the parameters of the RG (*r* and *m*), are matched to that experiment that generates the lowest value for the *PrE*.

Results

Quantitative results

- The optimal sizes for the expansion and erosion filters were (3,3,3) and (5,5,5), respectively. Regarding the trained LSSVM, values of 2.50 and 2.25 were obtained as optimal parameters for γ and σ^2, respectively. These parameters are found by means of the error that is presented when comparing the manual and automatic coordinates considering the percentage relative error (*PrE*). For this minimum value the *PrE*, the optimal values of RG's parameters, r and m, were 4 and 3.5, respectively.

- The best automatic segmentation of the meningioma yielded a value for its volume of 36.88 cm^3; while the volume associated with manual segmentation, of the aforementioned tumor, was 37.42 cm^3. This implies that the minimum *PrE* was 1.44%.

Qualitative results

Figure 5, shows a 2-D view of both the original MGT and the processed versions after applying the proposed technique.

Figure 5. Axial view of images belonging to DB1: a) Original, b) Erode, c) Gradient magnitude, d) Segmented with region growing technique, e) MGT Dilated.

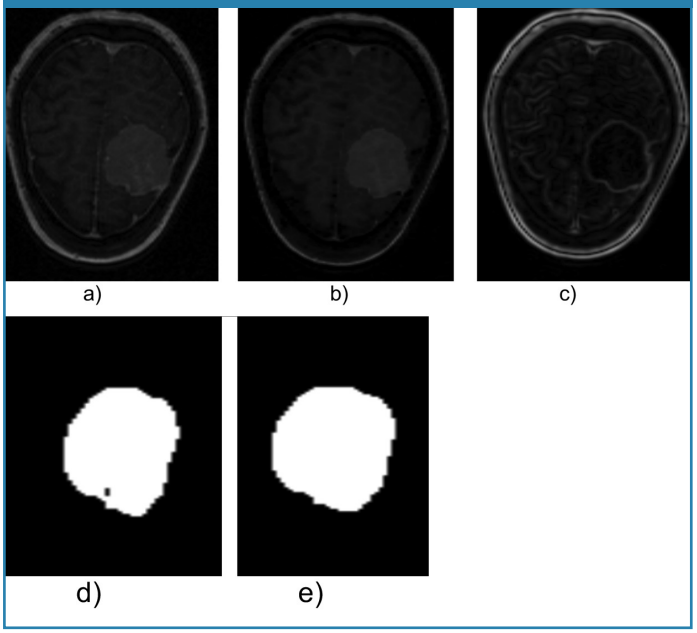

Conclusions

A computational technique has been displayed; its tuning process allows an accurate segmentation of a meningioma, presents in magnetic resonance images. This statement is supported by the fact that the *PrE* obtained was very low.

The use of intelligent operators, represented by the least squares vector support machines, allowed the automatic identification of the coordinates corresponding to the seed voxel which plays a crucial role in the adequate initialization of the unsupervised grouping algorithm based on region growing.

The meningioma volume is vital when deciding whether a patient is surgically treated or not. Both the size of a meningioma and its location can seriously compromise the health of a patient.

Computational techniques such as that developed in the present investigation are precise and useful to generate the exact location and precise quantification of the volume occupied by a tumor. Additionally, the meningioma segmentation is useful to plan surgery and to remove as much of the tumor as possible, while avoiding the excision of parts of the brain that control vital functions.

In the future, it is planned to carry out an inter-subject validation of the computational technique developed considering a significant number of three-dimensional images, linked to patients with this type of disease.

Acknowledgements
The authors are grateful for the financial support given by the Universidad Simón Bolívar-Colombia through the 2016-16 code project.

References

1. Stelzer K. Epidemiology and prognosis of brain metastases. Surg Neurol Int. 2013;4(Suppl 4):S192-202.
2. Mcneill KA. Epidemiology of Brain Tumors. Neurol Clin. 2016;34(4):981-998.
3. American Brain Tumor Association (ABTA). About Brain Tumors: A Primer for Patients and Caregivers. 9ª Edition. 2015 ABTA.
4. WHO (2007). Cavenee W, Louis D, Ohgaki H et al. Eds. WHO Classification of Tumours of the Central Nervous System. WHO Regional Office Europe.
5. Burger, Scheithauer, and Vogel, Surgical Pathology of the Nervous System and Its Coverings. 4th edition. Churchill Livingstone, Nueva York, 2002.
6. Vera M. Segmentación de estructuras cardiacas en imágenes de tomografía computarizada multi-corte. Ph.D. dissertation, Universidad de los Andes, Mérida-Venezuela, 2014.
7. Gudbjartsson H. y Patz S.The rician distribution of noisy MRI data, Magn. Reson. Med. 1995:34 (1):910-914.
8. Macovski A. Noise in MRI, Magn. Reson. Med. 1996:36 (1) 494-497.
9. Sanjuán A., Price C., Mancini L., Josse G., Grogan A., Yamamoto A., Geva S., Leff A., Yousry T., Seghier M. Automated identification of brain tumors from single MR images based on segmentation with refined patient-specific priors. Frontiers in Neuroscience. 2013:7(1):241-257
10. Hsieh T., Liu Y., Liao C., Xiao F., Chiang I., Wong J. Automatic segmentation of meningioma from non-contrasted brain MRI integrating fuzzy clustering and region growing. BMC Medical Informatics and Decision Making. 2011:11(1): 11-54.
11. Kaus M., Warfield S., Nabavi A., Chatzidakis E., Black P., Jolesz F. (1999). Segmentation of Meningiomas and Low Grade Gliomas in MRI. In Proceedings of Medical Image Computing and Computer-Assisted Intervention -- MICCAI'99. Kikinis R., Taylor, C. and Colchester A. editors. Springer Berlin Heidelberg. 1-10.
12. Serra J. Image Analysis Using Mathematical Morphology. London, England: Academic Press, 1982.
13. González R., Woods R. Digital Image Processing. USA: Prentice Hall, 2001.
14. Mukhopadhyay S., Chanda B. A multiscale morphological approach to local contrast enhancement. Signal Processing. 2000: 80(4): 685–696.
15. Yu Z., Wei G., Zhen C., Jing T., Ling L. Medical images edge detection based on mathematical morphology. In Proceedings of the IEEE Engineering in Medicine and Biology 27th Annual Conference, Shanghai–China, September 2005, pp. 6492–6495.
16. W. Pratt. Digital Image Processing. USA: John Wiley & Sons Inc, 2007.
17. Fischer M., Paredes J., Arce G. Weighted median image sharpeners for the world wide web. IEEE Transactions on Image Processing. 2002:11(7):717-27.
18. V. Vapnik, Statistical Learning Theory. New York: John Wiley & Sons, 1998.
19. E. Osuna, R. Freund, y F. Girosi. Training support vector machines: an application to face detection. In Conference on Computer Vision and Pattern Recognition (CVPR '97), San Juan, Puerto Rico, 1997, pp. 130–136.
20. A. Smola, "Learning with kernels," Ph.D Thesis, Technische Universitt Berlin,Germany, 1998.
21. B. Scholkopf y A. Smola, Learning with Kernels: Support Vector Machines, Regularization,Optimization, and Beyond. Cambridge, MA , USA: The MIT Press, 2002.
22. J. Suykens, T. V. Gestel, y J. D. Brabanter, Least Squares Support Vector Machines.UK: World Scientific Publishing Co., 2002.
23. M. Oren, C. Papageorgiou, P. Sinha, E. Osuna, y T. Poggio. Pedestrian detection using wavelet templates. In CVPR '97: Conference on Computer Vision and Pattern Recognition (CVPR '97). Washington, DC, USA: IEEE Computer Society, 1997, pp. 193–200.